


Temporospatial dynamics of the morphogenesis of the rabbit retina from prenatal to postnatal life: Light and electron microscopic study

Sara M. M. El-Desoky | Ruwaida Elhanbaly | Abdalla Hifny | Nagwa Ibrahim |
Wafaa Gaber 

Department of Anatomy and Embryology,
Faculty of Veterinary Medicine, Assiut
University, Assiut, Egypt

Correspondence

Wafaa Gaber, Department of Anatomy and
Embryology, Faculty of Veterinary Medicine,
Assiut University, Assiut 71526, Egypt.
Email: wafaa.anatomy@aun.edu.eg

Review Editor: Alberto Diaspro

Abstract

The retina consists of various cell types arranged in eight cell layers and two membranes that originate from the neuroectodermal cells. In this study, the timing of differentiation and distribution of the cellular components and the layers of the rabbit retina are investigated using light and electron microscopy and immunohistochemical techniques. There were 32 rabbit embryos and 12 rabbits used. The rabbit retina begins its prenatal development on the 10th day of gestation in the form of optic cup. The process of neuro- and gliogenesis occurs in several stages: In the first stage, the ganglionic cells are differentiated at the 15th day. The second stage includes the differentiation of Muller, amacrine, and cone cells on the 23rd day. The differentiation of bipolar, horizontal, and rod cells and formation of the inner segments of the photoreceptors consider the late stage that occurs by the 27th and 30th day of gestation. On the first week of age postnatally, the outer segments of the photoreceptors are developed. S100 protein is expressed by the Muller cells and its processes that traverse the retina from the outer to the inner limiting membranes. Calretinin is intensely labeled within the amacrine and displaced amacrine cells. Ganglionic cells exhibited moderate immunoreactivity for calretinin confined to their cytoplasm and dendrites. In conclusion, all stages of neuro- and gliogenesis of the rabbit retina occur during the embryonic period. Then, the retina continues its development postnatally by formation of the photoreceptor outer segments and all layers of the retina become established.

Research Highlights

- The aim of this study is to investigate the morphogenesis of the rabbit retina during pre- and postnatal life.
- The primordia of the retina could be observed in the form of the optic cup. The ganglionic cells are the first cells to differentiate, while the photoreceptor cells are the last.
- S100 protein is expressed by the Muller cells and its processes. Calretinin is intensely labeled in the amacrine and displaced amacrine cells and moderately expressed in the cytoplasm and dendrites of ganglionic cells.

KEYWORDS

calretinin, muller cells, optic cup, photoreceptors, S100

1 | INTRODUCTION

Rabbit's eyes sharing many histological and anatomical features with human and other domestic animals make their eyes suitable for ophthalmic surgical evaluation and for inspection of new ophthalmic surgical strategies (Gwon, 2008). Rabbit eyes are commonly used for experiments and assessing of ophthalmic drugs, so understanding of the histological development of the eye may help to identify time-sensitive point and effect of tissue differentiation exerted by drug administration (Kurata et al., 2017).

Concerning the eyeball, it consists of three concentric coats that are outer fibrous, middle vascular, and inner nervous coats. The retina is the neural layer of the eyeball that is about thin, delicate, transparent sheet. The retina plays a key role in vision as its primary function is image formation (Komáromy, 2010). Visual perception is a sensory process initiated at the retina and completed in the visual cortex of cerebrum (Tomar & Bansal, 2019).

The retina consists of various cell types arranged in eight cell layers and two membranes that are (rods and cones) internal limiting membrane, nerve fiber layer, ganglion cell layer, inner plexiform layer, inner nuclear layer, outer plexiform layer, outer nuclear layer, external limiting membrane, and inner and outer segments of photoreceptors. Light must traverse these many layers before initiating signal transduction in the rods and cones. Below the photoreceptors present the last layer that is the retinal pigment epithelium which consists of a monolayer of cuboidal cells containing many melanosomes from which the cells derive their pigmented color (Gupta, Herzlich, et al., 2016; Shara et al., 2013). A series of photoelectrical changes are responsible for the vision which occurs in various contributing cell types of retina. Hence, any change in its structure may lead to temporary or permanent blindness (Tomar & Bansal, 2019).

Development of the mammalian retina is a highly organized process which originating from neuroectodermal cells through induction of the optic pit, optic vesicle, and the optic cup (Miyata, 2008; Moshiri et al., 2004). The retina derives from the apposed walls of the optic cup. The cells of the outer layer of the optic cup form the retina pigmented epithelium. The inner layer of the optic cup differentiates into the neural retina (Gupta, Kapoor, et al., 2016).

Knowledge of induction, neuron proliferation, and differentiation of different cell types of retina are very important to explain the causes of some congenital anomalies that cause significant visual deficits as retinal separation and immaturation of photoreceptor cells (Sernagor et al., 2006).

The study of the retinal embryology is important to the field of development of the visual system (Greiner & Weidman, 1982). Many researchers study the origin, development, and structure of the retina for well over 100 years and yet many questions still remain to be answered before we can fully understand their biosynthesis and organization. Previous studies are targeting histological development of

the retina in many species of animals, but the information in rabbit eye still not yet available.

The retina has important roles in the process of vision; therefore, the purpose of this investigation is to evaluate the morphogenesis of the retina by using light and electron microscopy, as well as immunohistochemical techniques to provide a detailed analysis of retinal development and differentiation of white *New Zealand* rabbit.

2 | MATERIALS AND METHODS

The current study has been approved by the Ethical Committee of the Faculty of Veterinary Medicine, Assiut University, Assiut, Egypt, according to the OIE standards for use of animals in research under the No. 06/2022/0003.

2.1 | Sample collection

The current study was performed in accordance with the Egyptian Animals' laws and Ethics Committee of Assiut University, Faculty of Veterinary Medicine. This study was performed on 32 *New Zealand* white rabbit embryos obtained from the farm of Faculty of Agriculture, Assiut University. The age of fetuses and rabbits was estimated according to the records of the farm. The day of mating was considered the day one of embryonic life. The pregnant female rabbits were collected at different stages of pregnancy beginning from gestational days: 10, 11, 13, 16, 20, 23, 27, and 30 days. In addition, 12 *New Zealand* white rabbits were slaughtered at one and 2 weeks as well as the 1 month of postnatal life (four rabbits per age).

2.2 | Tissue preparation for paraffin embedding

The pregnant rabbits were slaughtered, and the embryos were removed. The rabbit embryos were processed as a whole, while at 23, 27, and 30 days, the head of the embryos was taken. In the postnatal ages, the eye ball only was collected. The collected samples were washed with normal saline solution (0.9%) NaCl and fixed immediately in 10% neutral buffered formalin at room temperature. Then, the fixed materials were dehydrated in ascending grades of ethanol, cleared in xylene, and impregnated with melted paraffin wax. Finally, paraffin blocks of the processed samples were prepared. Thin sections (5 μ m thick) were cut, dried in an electrical incubator, and stained with the following stains, according to Bancroft et al. (2013):

1. Harris hematoxylin and eosin for general inspection of the organs.
2. Combined Alcian blue-Periodic acid-Schiff (PAS) technique for detection of acidic and neutral mucopolysaccharides in retina.

2.3 | Scanning electron microscopy (SEM)

Representative samples from retina at 23 and 30 days of gestation and 1 week as well as 1 month of age postnatally were washed for several times in normal saline and acetic acid 2%, fixed in 4% glutaraldehyde solution for 24 h, and then post-fixed in 2% buffered osmium tetroxide. The fixed samples were washed in 0.1 M cacodylate buffer at PH 7.3 and then dehydrated in ascending grades of ethanol, critical point dried in liquid carbon dioxide, and mounted on metal stubs and then coated with gold palladium in sputtering device. The samples were examined and photographed by JEOL scanning electron microscope (JSM-5400 LV) operated at KV 10 in the Electronic Microscope Unit, Assiut University, Assiut, Egypt.

2.4 | Semithin sections and transmission electron microscopy (TEM)

Representative specimens from the fetuses at 23 and 30 days of gestation and 1 and 2 weeks as well as 1 month of age postnatally were used for semithin sections. Small pieces (2.0–3.0 mm long) from the specimens were placed on 2.5% cold glutaraldehyde in phosphate buffer (pH 7.2) for 24 h (Karnovsky, 1965). The pieces were washed twice in 0.1 M phosphate buffer and then post-fixed in 1% osmium tetroxide, in the same buffer. The post-fixed pieces were dehydrated in graded alcohols and embedded in araldite resin. Semi-thin sections (1 μ m) in thickness will be stained with 1% toluidine blue. Ultra-thin sections obtained by a Reichert ultra-microtome were stained with uranyl acetate and lead citrate (Reynolds, 1963) and examined under JOEL 100 II transmission electron microscope.

2.5 | Digitally colored TEM and SEM images

To increase the visual contrast between several structures on the same electron micrograph, we have digitally colored some cells, to make them more visible for the readers. The cells were carefully hand colored using Adobe Photoshop software version 6.

2.6 | Immunohistochemistry

Paraffin sections of (5 μ m) from retina at 23 and 30 gestational days and first and second weeks as well as the first month of age were

dewaxed by xylene, rehydrated by ascending grades of alcohol, and rinsed by PBS pH 7.4 (3 times for 5 min). Endogenous peroxidase was suppressed by using hydrogen peroxide block at room temperature. The sections were thoroughly washed by running tap water for an additional 10 min. To enhance antigen retrieval, the slides were treated with 10 mm sodium citrate buffer (pH 6.0) at temperature reached 95–98 in a water bath for 20 min. The sections were cooled for 20 min at room temperature and subsequently were washed in PBS (pH 7.4, 3 times for 5 min). Block non-specific background staining was performed by using Ultra V block, for 5 min at room temperature. Ultra V block application did not exceed 10 min to avoid staining artifact. The primary antibody was applied to the sections overnight at 4°C or 30–60 min at room temperature. The source, dilutions, and time of incubation of each antibody are shown in Table 1.

The slides were washed with PBS for 1 h at room temperature. Sections were washed using PBS (at pH 7.4, 3 times for 5 min). The biotinylated secondary antibody (Table 1) applied for 10 min at room temperature. Sections were washed by PBS (pH 7.4, 3 times for 5 min) and subsequently incubated with streptavidin-peroxidase complex for 10 min at room temperature. Visualization of the bound antibodies was performed using 1 drop of DAB plus chromogen to 2 mL of DAB plus substrate. The mixture was applied and incubated at room temperature for 5 min. The incubation processes were carried out in a humid chamber. Harris hematoxylin was used as counters stained for 30s. The sections were dehydrated using ethanol and isopropanol I and II, cleared in xylene, and covered by DPX (Abd-Elhafeez & Soliman, 2017; Abdel-Maksoud et al., 2019).

The expressions of calretinin and S100 protein in the retina were examined microscopically using OLYMPUS BX51 microscope, and the images were taken using OLYMPUS DP72 camera adapted to the microscope. Assessing the intensity of the immunostaining, the staining of the nucleus and/or cytoplasm by the following amount and color of immunostaining: strong (dark brown to black), moderate (brown), mild (light brown), and negative immunostaining (no immunoreactivity) (Abd-Elkareem, 2017).

2.7 | Morphometric analysis

Images of semithin sections of the 30th prenatal age, in addition to the 1st and 2nd week and the 1st month postnatal ages, were used for morphometric assessments using ImageJ software (1.51w, Wayne Rasband, National Institutes of Health, USA). The thickness (μ m) of the different layers of the rabbit retina (inner nuclear layer, outer

TABLE 1 The source, dilution, and time of incubation of the antibodies used in the immunohistochemical studies.

Target	Primary antibody supplier	Origin (catalog no.)	Dilution	Incubation	Ag retrieval	Biotinylated secondary antibody
Calretinin (H-5)	Diagnostic BioSystems	Mouse (MC; Mob593)	1:25	30–60 min at RT	Microwave	Rabbit anti mouse IgG
S100 Protein	Diagnostic BioSystems	Rabbit (PC; RP035)	1:50	30 min at RT	Microwave	Goat anti rabbit IgG

Note: MC (monoclonal), PC (polyclonal), RT (room temperature), and m (microwave heating in citrate buffer (pH 6.0), 3 \times 10 min. From ThermoFisher Scientific/Lab Vision, Fremont, CA, USA. Diagnostic BioSystems, Emργο Europe.

nuclear layer, inner plexiform layer, outer plexiform layer) was measured. All these measurements were performed on three randomly selected sections per developmental age (from each section, three randomly selected regions were measured). In addition, the thickness (μm) of the inner and outer layers of the optic cup was measured using images of stained paraffin sections of the 10th prenatal age. The values were expressed as the mean \pm standard deviation (SD).

3 | RESULTS

On the 10th day of gestation, the optic cup is formed consisting of inner and outer layers separated by a wide cavity representing the

prospective intra-retinal space. The epithelium of the two layers is stratified. The inner layer is thicker (8.24 ± 0.92) and invaginates toward the outer one (4.97 ± 0.32) (Figure 1a). On the 11th day, the optic cup could be observed connecting with the diencephalon through the optic stalk. The epithelium lining the optic stalk is stratified (Figure 1b). The epithelium of the outer layer of the optic cup becomes simple consisting of single layer of columnar to cuboidal cells, which represents the prospective pigmented layer of the retina. The epithelium of the inner layer remains stratified, representing the prospective nervous layer of the retina. The innermost nuclei of this layer are shifted basally (Figure 1c).

On the 13th day of gestation, the inner layer of the optic cup could be subdivided into two parts: large posterior pars optica and

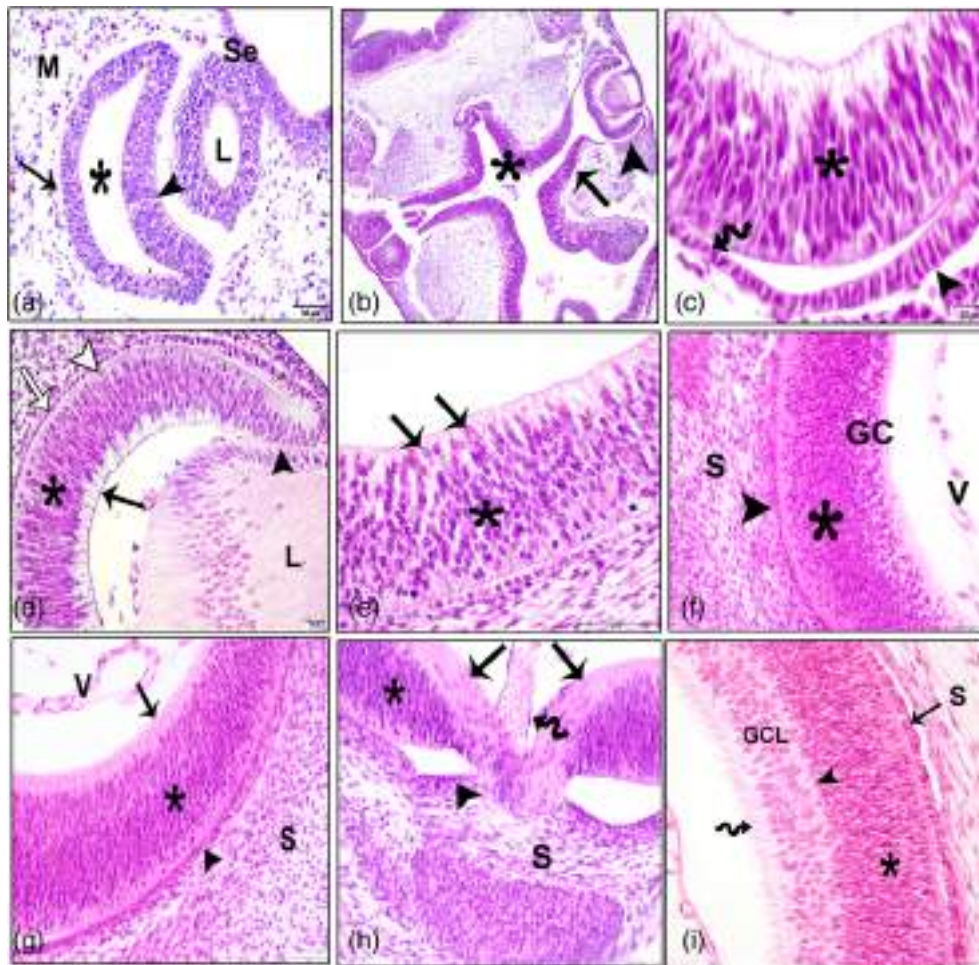


FIGURE 1 Paraffin sections of embryonic rabbit eyes stained with hematoxylin and eosin. (a) 10th gestational day, the inner layer (arrowhead) and the outer layer (arrow) of the optic cup are separated by a wide cavity (asterisk). Surface ectoderm (Se), lens (L), and surrounding mesenchyme (M). (B, C) 11th gestational day. (b) Showing the optic cup (arrowhead) is connected with the diencephalon (asterisk) through the optic stalk (arrow). (c) The outer layer of the optic cup becomes columnar (arrowhead) to cuboidal (zigzag arrow) cells. The inner layer of the optic cup (asterisk). (d) 13th gestational day, the pars theca (arrowhead), pars optica that consisted of inner marginal layer (arrow) and outer neuroblastic cell layer (asterisk). Notice, mitotic figures (white arrowhead), retinal pigmented epithelium (white arrow), and lens (L). (e) On the 15th gestational day, the ganglionic cells (arrows) are represented by the innermost cell bodies of the neuroblastic cell layer (asterisk). (F–H) 16th gestational day. (f): The ganglionic cells (GC) and the neuroblastic cell mass (asterisk). (g, h) The nerve fiber layer (arrow) converges to form the optic nerve enclosing the hyaloid artery (zigzag arrow). Vitreous chamber (V), retinal pigmented epithelium (arrowhead), and sclera (S). (i) 20th gestational day inner ganglionic cell layer (GCL), outer neuroblastic cell layer (asterisk), and inner plexiform layer (arrowhead). Retinal pigmented epithelium (arrow), nerve fiber layer (zigzag arrow), and sclera (S).

small anterior pars theca without a definite demarcation. The pars optica consists of two layers: inner thin anuclear marginal layer and outer thick neuroblastic cell layer. The pars theca is thin and is uniformly nucleated throughout its thickness (Figure 1d). On the 15th day, the ganglionic cells begin to appear at the center of the retina. They are represented by the innermost cell bodies of the neuroblastic cell layer which become less basophilic than the other neuroblastic cells (Figure 1e).

On the 16th day of gestation, the ganglionic cells are loosely arranged along the entire length of the retina (Figure 1f). The nerve fiber layer could be observed at this age and is represented by the long axonic processes of the ganglionic cells that extend over the inner surface of the retina and converge centrally to form the optic nerve enclosing the hyaloid artery (Figure 1g,h).

On the 20th day of gestation, the neuroblastic cell mass could be divided into an inner ganglionic cell layer and an outer neuroblastic cell layer separated by a space. This space is occupied by a network of fibers and represents the inner plexiform layer. Some migrated cells could be seen crossing the inner plexiform layer (Figure 1i). The ganglionic cell layer is multilayered and characterized by large cells with light staining nuclei. The neuroblastic cell layer is composed of smaller, densely packed cells with darkly stained nuclei.

On the 23rd day of gestation, the neural retina consists of inner limiting membrane, nerve fiber layer, ganglionic cell layer, inner plexiform layer, and neuroblastic cell layer (Figure 2a). The inner limiting membrane which is the innermost layer of the neural retina could be detected at this age showing positive reaction for Alcian blue (Figure 2b). Within the nerve fiber layer, the Muller cells could be

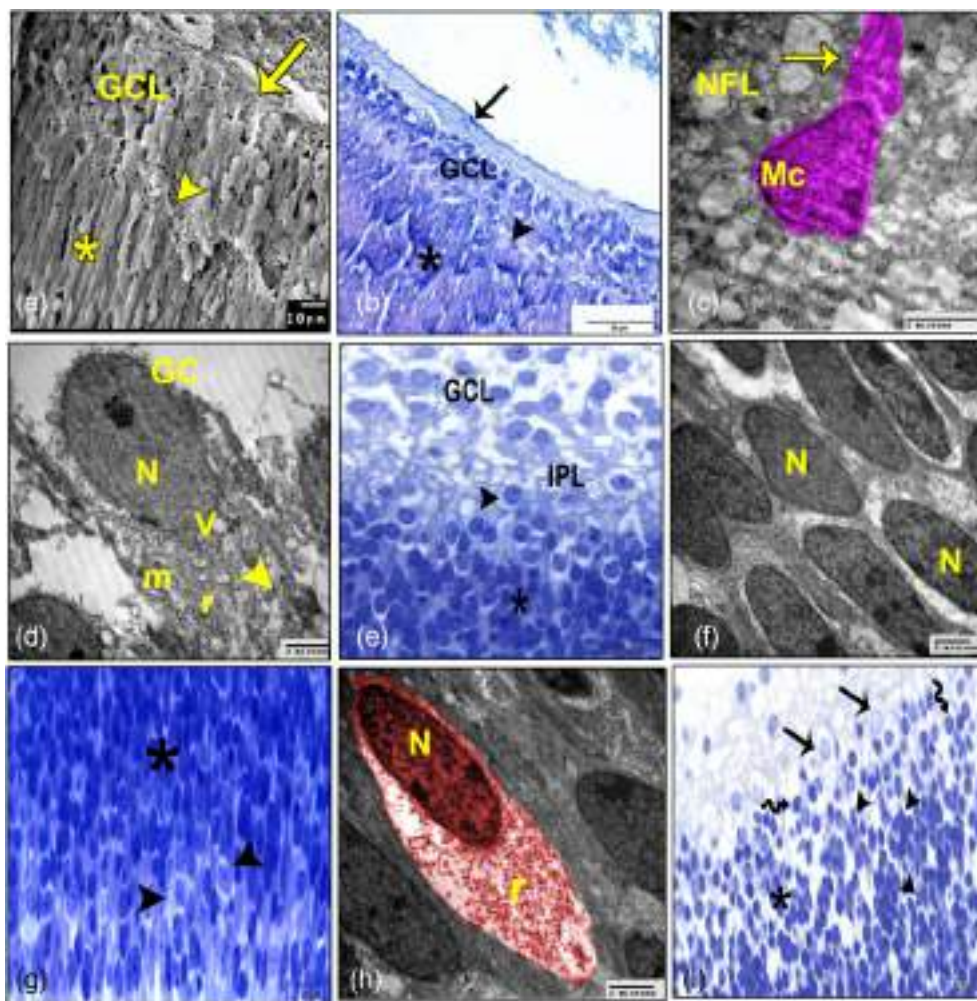


FIGURE 2 (A–H) 23rd gestational day. (a) SEM of nerve fiber layer (arrow), ganglionic cell layer (GCL), inner plexiform layer (arrowhead), and neuroblastic cell layer (asterisk). (b) Paraffin section stained with Alcian blue/PAS stain showing the inner limiting membrane (arrow) reacted positively with Alcian blue, ganglionic cell layer (GCL), inner plexiform layer (arrowhead), and neuroblastic cell layer (asterisk). (c) Digitally colored TEM showing the Muller cell (MC, violet) and its radial process (arrow) within the nerve fiber layer (NFL). (d) TEM of the ganglionic cells (GC). Nucleus (N), vesicles (V), mitochondria (m), rough endoplasmic reticulum (arrowhead), and ribosomes (r). (e) Semithin section showing the amacrine cells (arrowhead), the neuroblastic cell layer (asterisk), and the inner plexiform layer (IPL). (f) TEM of neuroblastic cells is fusiform in shape with ovoid nucleus (N). (g) Semithin section shows the cone cells (arrowheads) at the outer margin of the neuroblastic cell layer (asterisk). (h) Digitally colored TEM of the cone cell (red). Nucleus (N) and free ribosomes (r). (i) 27th gestational day, semithin section showing the differentiated cells in the neuroblastic cell layer (asterisk). Amacrine cells (arrows), Muller cells (arrowheads), and bipolar cells (zigzag arrows).

observed having intensely stained angular nuclei and thick radial processes (Figure 2c).

The ganglionic cells appear as large oval cells containing oval euchromatic eccentric nucleus with prominent nucleolus. The cytoplasm contains free ribosomes, mitochondria, rough endoplasmic reticulum (rER), and few vesicles (Figure 2d). In the neuroblastic cell layer, the amacrine cells observed toward the inner plexiform layer. They are large rounded cells with distinct nucleus and lightly stained cytoplasm (Figure 2e). The undifferentiated cells of the neuroblastic cell layer are arranged in longitudinal rows. They are fusiform in shape with ovoid nuclei occupy most of the cell body (Figure 2f). Toward the outer margin of the neuroblastic cell layer, the prospective cone cells appear as large pale oval cells. These cells have an oval heterochromatic eccentric nucleus and electron lucent cytoplasm filled with free ribosomes (Figure 2g,h).

On the 27th day of gestation, the Muller and bipolar cells could be observed within the neuroblastic cell layer. The Muller cell appears as small, elongated darkly stained cells. The bipolar cells appear as small and rounded with darkly stained nuclei (Figure 2i).

At the end of gestation, specifically on the 30th gestational day, two types of ganglionic cells could be distinguished: large ganglionic cells with large pale nucleus and small ganglionic cells with small darkly stained nucleus (Figure 3a). Ultrastructurally, the ganglionic cell has rounded eccentric nucleus and its cytoplasm contains vesicles that

are accumulated in the marginal zone forming a conical outpouching (Figure 3b). The inner plexiform layer becomes a distinct layer. The neuroblastic cell layer is divided into inner and outer nuclear layers. The outer plexiform layer appears as a faint line of separation that demarcates the inner nuclear layer from the outer nuclear layer (Figure 3c, Table 2).

The inner part of the inner nuclear layer contains more differentiated, lighter, and less condensed cells. These differentiated cells are amacrine, bipolar, and Muller cells, while the horizontal cells are observed toward the outer margin of the inner nuclear layer (Figure 3d). Ultrastructurally, the amacrine cell has heterochromatic nucleus and wide cytoplasmic processes that contain free ribosomes, RER, mitochondria, SER, and vesicles (Figure 3e). The bipolar cell bodies are ovoid in shape with large rounded to oval-shaped nucleus surrounded by thin rim of cytoplasm. The Muller cell has electron dense heterochromatic oval- or triangular-shaped nucleus. Thin and long cytoplasmic processes extend from the cell bodies and are lodged between the other cells (Figure 3f).

The horizontal cells appear as large, light staining cells that are interspersed between the darker undifferentiated cells of the outermost row of the inner nuclear layer (Figure 4a). Ultrastructurally, the horizontal cell appears as large, electron lucent pyramidal-shaped cell. It has an euchromatic eccentric nucleus and abundant of cytoplasm rich in free ribosomes, mitochondria, and vesicles (Figure 4b).

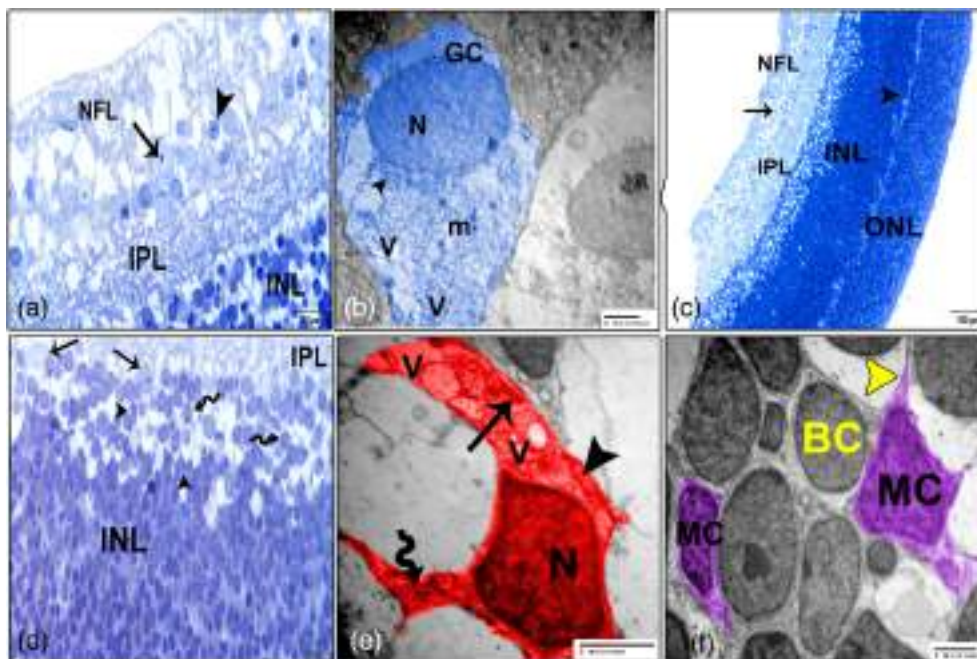


FIGURE 3 Neural retina on the 30th gestational day. (a) Semithin section showing large ganglionic cell (arrow), small ganglionic cell (arrowhead), nerve fiber layer (NFL), inner plexiform layer (IPL), and inner nuclear layer (INL). (b) Digitally colored TEM showing the ganglionic cell (GC, blue), nucleus (N), mitochondria (m), rough endoplasmic reticulum (arrowhead), and abundant of vesicles (V). (c) Semithin section showing the nerve fiber layer (NFL), ganglionic cell layer (arrow), inner plexiform layer (IPL), inner nuclear layer (INL), outer plexiform layer (arrowhead), and outer nuclear layer (ONL). (d) Semithin section shows the inner nuclear layer (INL), amacrine cells (arrows), Muller cells (arrowheads), and bipolar cells (zigzag arrows). (e) Digitally colored TEM of the amacrine cells (AC, red), nucleus (N), and cytoplasmic processes that contain rough endoplasmic reticulum (arrow), mitochondria (zigzag arrow), vesicles (V), and smooth endoplasmic reticulum (arrowhead). (f) Digitally colored TEM of the bipolar cells (BC, yellow) and Muller cells (MC, violet) and cytoplasmic processes of Muller cells (yellow arrowheads).

TABLE 2 Thickness of the different layers of the rabbit retina in various developmental ages.

Age	Inner nuclear layer	Outer nuclear layer	Inner plexiform layer	Outer plexiform layer
30th day of gestation	4.32 ± 0.03	2.98 ± 0.09	1.11 ± 0.1	-
1 week postnatally	2.74 ± 0.1	2.91 ± 0.04	1.45 ± 0.05	0.31 ± 0.05
2 weeks	1.28 ± 0.01	2.42 ± 0.08	1.51 ± 0.05	0.57 ± 0.03
1 month	0.74 ± 0.07	1.59 ± 0.07	1.53 ± 0.01	0.58 ± 0.04

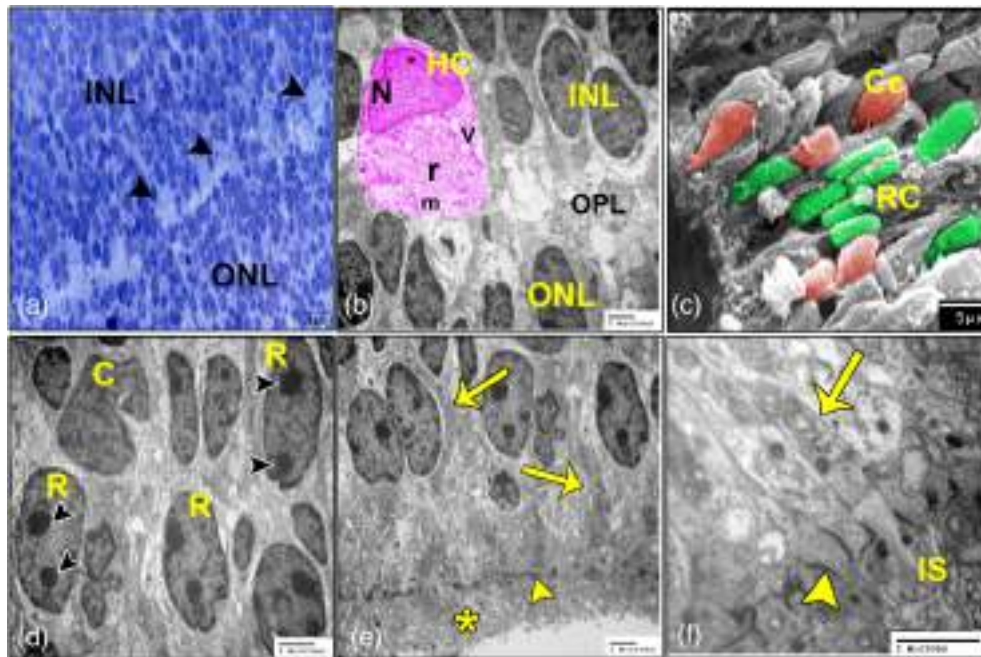


FIGURE 4 Neural retina on the 30th gestational day. (a) Semithin section shows the horizontal cells (arrowheads), inner nuclear layer (INL), and outer nuclear layer (ONL). (b) Digitally colored TEM of the horizontal cell (HC, pink), nucleus (N), free ribosomes (r), mitochondria (m), and vesicles (V) and outer plexiform layer (OPL). (c) Digitally colored SEM showing the rod cells (RC, green) and the cone cells (Cc, brown). (d) TEM of the rods (R) and cones (C), two distinct nucleoli (arrowheads) in the rod nucleus. (e) TEM of the processes of the Muller cells (arrows) between the photoreceptor cells, the outer limiting membrane (arrowhead), and inner segments of the photoreceptors (asterisk). (f) Higher magnification showing the outer limiting membrane (arrowhead) between the processes of the muller cells (arrow) and the inner segments of the photoreceptors (IS).

The outer nuclear layer contains the differentiated cell bodies of the photoreceptors (rods and cones). The cone cells have large cone shape, and their nuclei are large and heterochromatic. The rod cells have small elongated cylindrical shape, and their nuclei are elongated, heterochromatic with two distinct nucleoli (Figure 4c,d). The processes of the Muller cells could be observed between the photoreceptor cells. These processes are filled with mitochondria and extend to form the outer limiting membrane. The outer limiting membrane could be seen as electron dense line representing the zonula adherence between the processes of the Muller cells and between these processes and the inner segments of photoreceptor cells. Outpouchings from the developing photoreceptor cells could be observed extending beyond the outer limiting membrane. These outpouchings consider the earliest stage in the development of the inner segments of photoreceptors (Figure 4e,f).

In the one-week-old rabbits, the ganglionic cell layer becomes a single layer of ganglionic cells (Figure 5a). These cells increase in their

cytoplasmic volume that contains a profuse of vesicles, free ribosomes, and clusters of rough endoplasmic reticulum forming Nissl bodies (Figure 5b). The inner plexiform layer becomes thicker and gives positive reaction for Alcian blue (Figure 5c, Table 2).

All cells of the inner nuclear layer become differentiated (Figure 5d). Ultrastructurally, the amacrine cells are characterized by large deeply indented nuclei with eccentric nucleolus. Their electron dense cytoplasm contains RER, SER, mitochondria, and free ribosomes (Figure 5e). Two types of bipolar cells could be observed at this age: large pale cells with large euchromatic nuclei and distinct nucleoli that are distributed throughout the inner nuclear layer, representing the cone bipolar cells, and small dark cells with heterochromatic nuclei that are mostly concentrated toward the outer plexiform layer, representing the rod bipolar cells (Figure 5f,g). The Muller cells are characterized by an angular euchromatic nucleus surrounded with thin rim of dense cytoplasm. The cytoplasm extends radially forming processes containing SER, mitochondria, vesicles, and free ribosomes

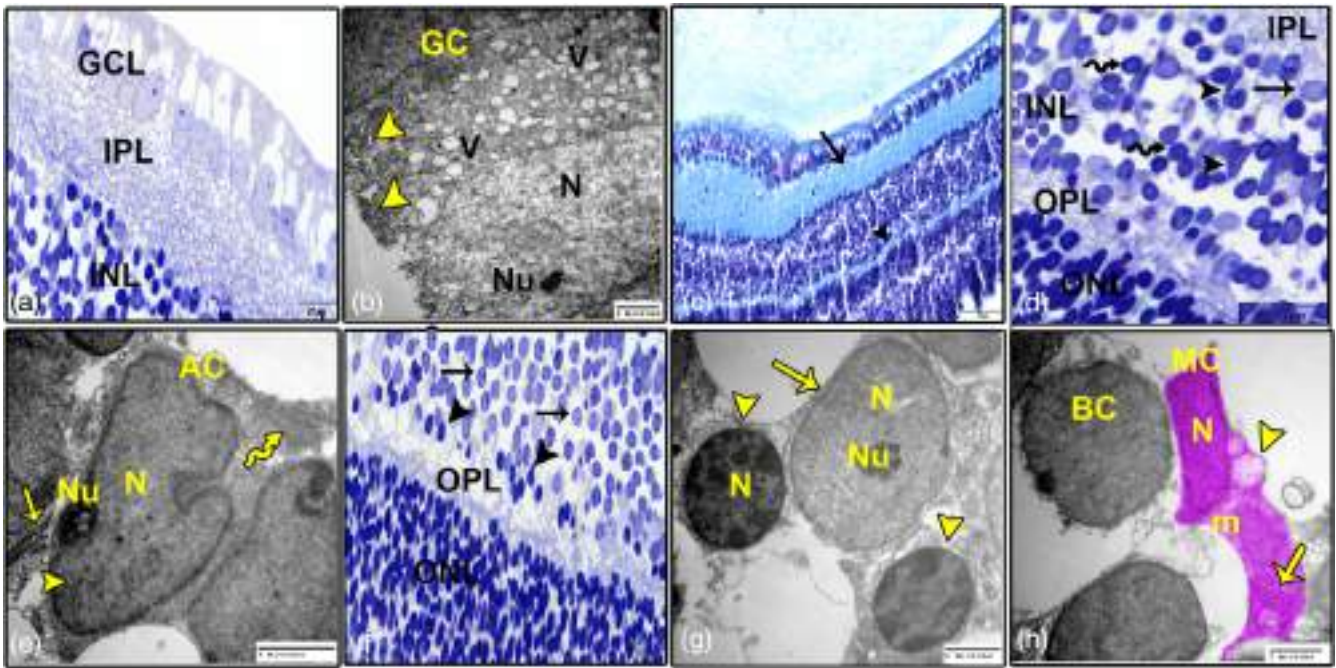


FIGURE 5 Neural retina of 1-week-old rabbit. (a) Semithin section showing the ganglionic cell layer (GCL), inner plexiform layer (IPL), and the inner nuclear layer (INL). (b) TEM shows the ganglionic cells (GC), nucleus (N), nucleolus (Nu), vesicles (V), and Nissl bodies (arrowheads). (c) Paraffin section stained with Alcian blue/PAS stain showing positive reaction for Alcian blue in the inner plexiform layer (arrow) and the outer plexiform layer (arrowhead). (d) Semithin section showing the cells of the inner nuclear layer (INL), Amacrine cells (arrow), Muller cells (arrowheads), bipolar cells (zigzag arrows), inner plexiform layer (IPL), outer plexiform layer (OPL), and outer nuclear layer (ONL). (e) TEM shows the amacrine cell (AC), nucleus (N), nucleolus (Nu), rough endoplasmic reticulum (arrow), smooth endoplasmic reticulum (zigzag arrow), and mitochondria (arrowhead). (f) Semithin section and (g) TEM image shows the cone bipolar cells (arrows), rod bipolar cells (arrowheads), nucleus (N), nucleolus (Nu), outer plexiform layer (OPL), and outer nuclear layer (ONL). (h) Digitally colored TEM showing the Muller cell (MC, violet), nucleus (N), vesicles (arrowhead), mitochondria (m), smooth endoplasmic reticulum (arrow), and bipolar cell (BC).

(Figure 5h). The nucleus of the horizontal cells greatly enlarges, occupies most of the cell, and is surrounded by a thin rim of cytoplasm from which the horizontal cell processes extend (Figure 6a).

The outer cells of the outer nuclear layer are more differentiated than the inner ones which situate close to the outer plexiform layer (Figure 6b). In the cone cells, the nuclei have evenly distributed chromatin, while in the rod cells, the chromatin is condensed in zones (Figure 6c,d). The photoreceptor layer is differentiated into inner and outer segments. The inner segments are more developed and consist of two parts: inner myoid and outer ellipsoid. The inner myoid part contains free ribosomes and Golgi apparatus, while the outer ellipsoid part is filled with mitochondria. The outer segments begin to develop at this age as disc-like infoldings of the plasma membrane. Basal bodies of the connecting cilia could be observed between the inner and outer segments (Figure 6e–g).

The Bruch's membrane could be observed at this age. It is represented by the basement membrane of the retinal pigmented epithelium (Figure 6h). In the two-week-old rabbits, the Bruch's membrane becomes a distinct line that is consisted of the basement membrane of the retinal pigmented epithelium and of the choroid capillaries (Figure 6i).

In the one-month-old rabbits, all layers of the retina are established. These layers are inner limiting membrane, nerve fiber layer, ganglionic cell layer, inner plexiform layer, inner nuclear layer, outer

plexiform layer, outer nuclear layer, outer limiting membrane, photoreceptor layer, and retinal pigmented layer (Figure 7a,b, Table 2).

The inner limiting membrane is a basement membrane that is formed by the radial processes of the Muller cells. The nerve fiber layer is formed by the axons of the ganglionic cells. The ganglionic cell layer is formed of a single row of two types of ganglionic cells: large ganglionic cells and small ganglionic cells. The inner plexiform layer is a thick complicated layer that situates between the ganglionic cell layer and inner nuclear layer (Figure 7c,d).

The inner nuclear layer is located between the inner and outer plexiform layers containing about three rows of cells. The cellular components of the inner nuclear layer are the amacrine, bipolar, Muller, and horizontal cells. These cells are different in shapes, sizes, and stain intensity. The amacrine cells occupy the innermost portion of the inner nuclear layer (Figure 7e,f). The cytoplasmic processes of the Muller cells are radiated and form multiple recesses where the bodies of the bipolar cells are enclosed (Figure 8a,b). The horizontal cells occupy the outermost portion of the inner nuclear layer (Figure 7e).

The outer plexiform layer is a thin layer that separates the outer and inner nuclear layers (Figure 8c). The outer nuclear layer is formed mainly of cell bodies of the photoreceptor cells (rods and cones). They are arranged in longitudinal columns; each column contains about 6–7 cells. These cells have darkly stained nuclei with minimal intercellular

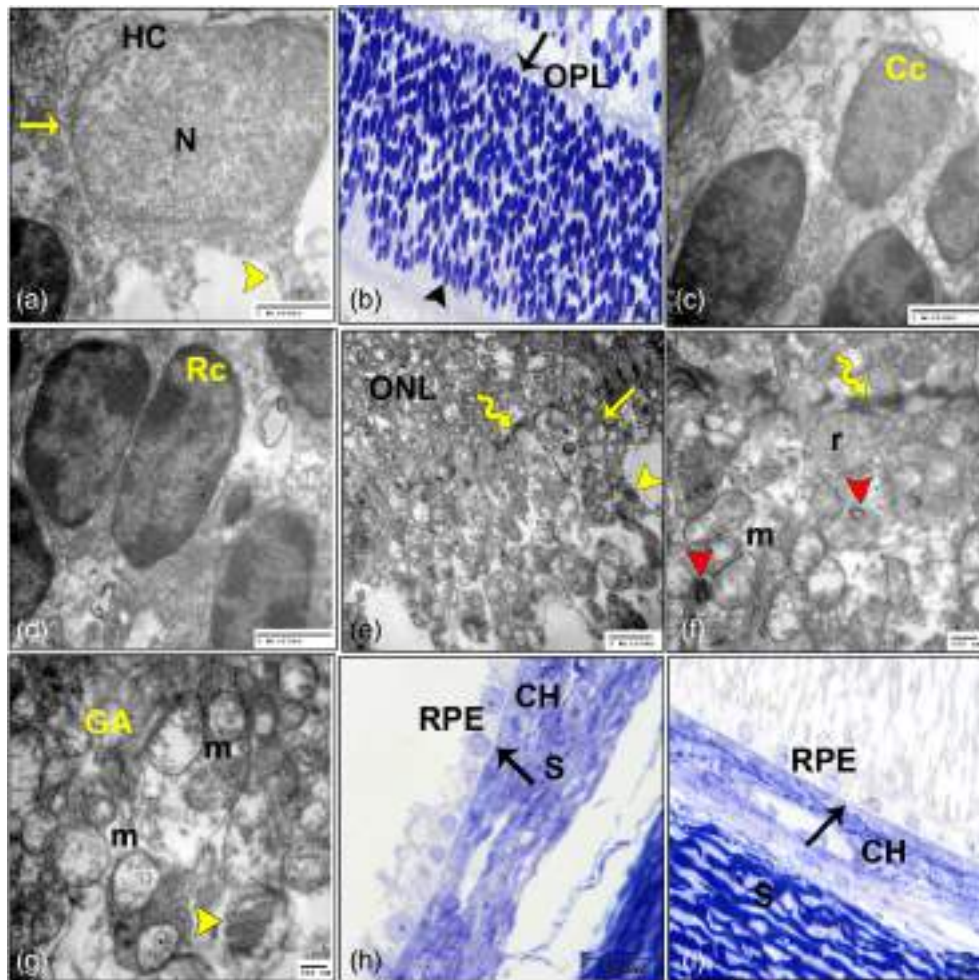


FIGURE 6 Neural retina of 1-week-old rabbit. (a) TEM showing the horizontal cell (HC) with its process (arrowhead), large nucleus (N), and thin rim of cytoplasm (arrow). (b) Semithin section shows the outer (arrowhead) and inner cells (arrow) of the outer nuclear layer and outer plexiform layer (OPL). (c) TEM showing the nuclei of the cone cells (Cc). (d) TEM showing the nuclei of the rod cells (Rc). (e) TEM showing the inner segments (arrow) and outer segments (arrowhead) of the photoreceptor layer, outer limiting membrane (zigzag arrow), and outer nuclear layer (ONL). (f, g) TEM of the inner and outer segments of the photoreceptors showing outer limiting membrane (zigzag arrow), mitochondria (m), free ribosomes (r), basal bodies of the connecting cilia (red arrowheads), Golgi apparatus (GA), and outer segment (arrowhead). (h) Semithin section showing the Bruch's membrane (arrow), retinal pigmented epithelium (RPE), choroid (Ch), and sclera (S). (i) Developing retina of 2-week-old rabbit shows the distinct Bruch's membrane (arrow) between the retinal pigmented epithelium (RPE) and the choroid (Ch) and sclera (S).

spaces (Figure 8c,d). The outer limiting membrane appears as an undulating line, separating the outer nuclear layer from the photoreceptor layer (Figure 8e). The inner segments of photoreceptor cells are long, condensed and contain elongated mitochondria with intact cristae. The outer segments increase in length. These segments arrange into stacks and appear as elongated, straight, cylindrical structures. They contain flattened, horizontal, lamellar discs formed by infoldings of their plasma membrane (Figure 8f).

3.1 | S100 immunohistochemical analysis

S100 protein is expressed in the retinal glial cells. Glial cells showed strong positive reaction for this protein in the nucleus and cytoplasm as well as their processes. Astrocytes are localized in the nerve fiber layer. Positively stained satellite glial cells could be observed

surrounding the ganglionic cells which showed negative immunoreactivity for S100. Intensely stained cell bodies of Muller cells could be observed within the inner nuclear layer. The radiating processes of Muller cells could be seen traversing the retina from the inner limiting membrane to the outer limiting membrane. These processes cross the inner plexiform layer, surround the ganglionic cells, and extend into the nerve fiber layer to reach the inner limiting membrane. In the same way, they cross the outer plexiform layer and extend between the cells of the outer nuclear layer to reach the outer limiting membrane (Figure 9).

3.2 | Calretinin immunohistochemical analysis

Amacrine cells within the inner nuclear layer and the displaced amacrine cells in the ganglionic cell layer showed strong positive reaction

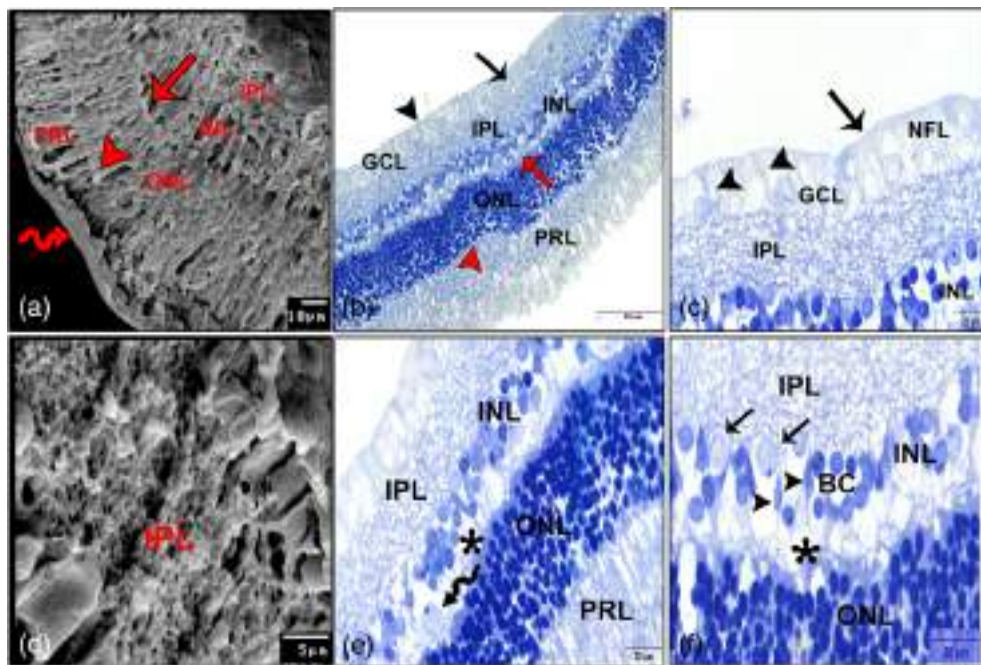


FIGURE 7 Developing retina of 1-month-old rabbit. (a) SEM image and (b) semithin section showing all layers of the retina. Inner limiting membrane (arrowhead), nerve fiber layer (arrow), ganglionic cell layer (GCL), inner plexiform layer (IPL), inner nuclear layer (INL), outer plexiform layer (red arrow), outer nuclear layer (ONL), outer limiting membrane (red arrowhead), photoreceptor layer (PRL), and retinal pigmented epithelium (zigzag arrow). (c) Semithin section shows the inner limiting membrane (arrow), the processes of Muller cells (arrowheads), nerve fiber layer (NFL), ganglionic cell layer (GCL), inner plexiform layer (IPL), and inner nuclear layer (INL). (d) SEM showing the thick inner plexiform layer (IPL). (e, f) Semithin sections showing the cellular components of the inner nuclear layer (INL), amacrine cells (arrows), Muller cells (arrowheads), bipolar cells (BC), horizontal cell (zigzag arrow), inner plexiform layer (IPL), outer plexiform layer (asterisk), outer nuclear layer (ONL), and photoreceptor layer (PRL).

for calretinin. Immunoreactivity for calretinin is expressed in the nucleus, cytoplasm, and the processes of these cells. Ganglionic cells exhibited moderate immunoreactivity for calretinin confined to their cytoplasm and dendrites, whereas the nuclei of ganglionic cells presented negative reaction. Processes of the amacrine cells and dendrites of the ganglionic cells form a positively stained meshwork within the inner plexiform layer (Figure 10).

4 | DISCUSSION

Throughout this investigation, we documented the timing of differentiation of all cells and layers of the rabbit retina and summarized in Table 3.

The primordia of the rabbit retina appear as optic cup is composed of inner and outer layers. The outer layer of the optic cup is early differentiated into the pigmented layer of the retina on 11th day of gestation. This agrees with Kuwabara and Weidman (1974) in rat, that the differentiation of the retinal pigmented epithelium (RPE) appears earlier than that of the neural retina. The RPE is separated from the underlying choroid by the Bruch's membrane (Masland, 2001). Gupta, Kapoor, et al. (2016) interpret that the Bruch's membrane is made up of basement membrane of the RPE only at first. Then, it is formed with the contribution from the choroidal capillaries. Defects

within the Bruch's membrane enhance the growth of the choroidal vessels into the subretinal space in choroidal neovascularization (Masland, 2001). The RPE assists to nourish the overlying neurosensory retina (Masland, 2001; Wassle & Boycott, 1991).

The inner layer of the optic cup undergoes a complicated process of differentiation into a multilayered neural retina (McGeady et al., 2006). The differentiation of neural retina begins by ganglionic cells differentiation. We are in agreement with Walsh and Polley (1985) in cat and Rapaport et al. (2004) in rat that the small retinal ganglionic cells are generated early and increase in size at developmental stage. After the differentiation of the ganglionic cell layer, the inner layer of the optic cup can be considered as neural retina (Carlson, 1985). The ganglionic cells begin to decrease in number until become a single cell thick of ganglionic cells, this result is agreed with Greiner and Weidman (1981) in rat and Gupta, Kapoor, et al. (2016) in human. Our investigation revealed that there are two types of ganglionic cells: large light and small dark cells. This resembles that described by Harman et al. (2001) in camel and Ehrenhofer et al. (2002) in equine. On the other hand, Boycott and Wassle (1974) described three types of ganglionic cells in cat retina: α , β , and γ .

Concerning the inner plexiform layer (IPL), it represents by the connections between axons of the bipolar cells, processes of amacrine cells, and the dendrites of the ganglionic cells and it continues increase in thickness as a result of axon growth and dendritic

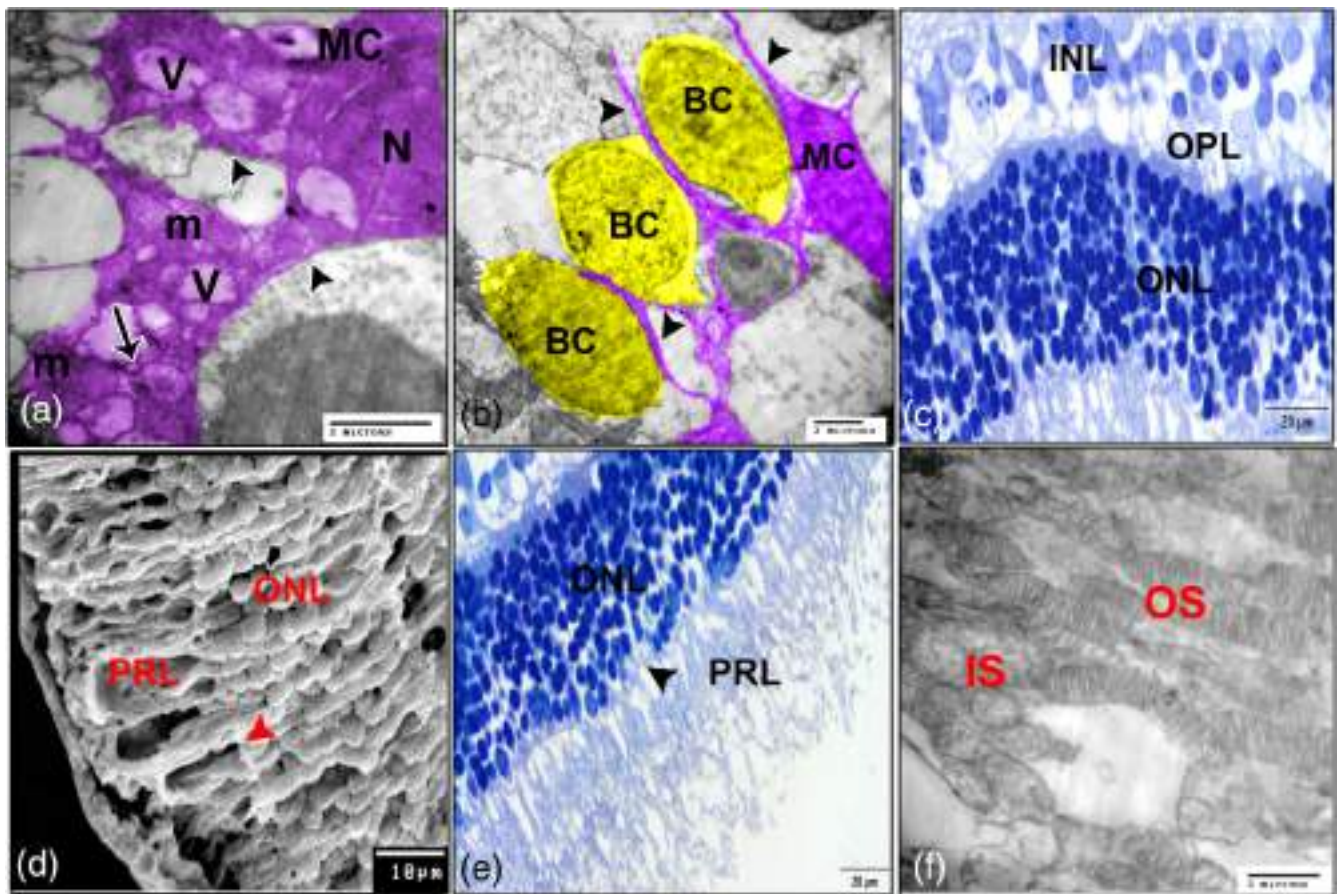


FIGURE 8 Neural retina of 1-month-old rabbit. (a, b) Digitally colored TEM showing the Muller cells (MC, violet) and the bipolar cells (BC, yellow), nucleus (N), cytoplasmic processes (arrowheads), mitochondria (m), vacuoles (V), and rough endoplasmic reticulum (arrow). (c) Semithin section and (d) SEM image showing the outer nuclear layer (ONL), inner nuclear layer (INL), outer plexiform layer (OPL), outer limiting membrane (arrowhead), and photoreceptor layer (PRL). (e) Semithin section showing the outer limiting membrane (arrowhead) separates the outer nuclear layer (ONL) from the photoreceptor layer (PRL). (f) TEM showing the inner segments (IS) and outer segment (OS) of the photoreceptor layer.

arborization (Walling & Marit, 2016). The inner nuclear layer (INL) becomes a distinct layer at the end of gestation and begins to separate from the outer nuclear layer (ONL) by appearance of the outer plexiform layer (OPL). The Muller cells are the earliest cell among the cells of the INL to differentiate and appear along the vitreal border of the retina in mice. Then, the Muller cells migrate outwardly and become scattered throughout the depth of the retina (Bhattacharjee & Sanyal, 1975).

Within the cytoplasmic processes of the Muller cell, abundant of mitochondria observed and it considers the source of energy. The Muller cell functions require considerable energy production, and previous literature has primarily emphasized glycolysis as the main energy provider. However, recent studies highlight the need of mitochondrial ATP production to upheld Muller cell functions (Toft-Kehler et al., 2017). Muller glia regulates neuronal development via phagocytosis of cellular debris including apoptotic cells and synapses (Tworig & Feller, 2021). Also, the Muller cell creates the acellular fibrous internal limiting membrane and supports the inner segments of the photoreceptors (Masland, 2001). Some studies confirm the Muller cells have regenerative capacity in retinal mouse and rat that

can reenter the cell cycle in response to injury and give rise to retinal neurons (Fischer & Bongini, 2010; Haruta et al., 2004; Hitchcock & Raymond, 2004). Among multiple functions, Muller cells are responsible for the removal of neurotransmitters, buffering potassium, and providing neurons with essential metabolites (Toft-Kehler et al., 2017).

Through this developmental study, we found that the amacrine cells not change its position. It remains occupying the inner margin of the inner nuclear layer. This simulated that described by Soliman et al. (2010) in goat. The amacrine cells can synapse back onto bipolar cells, other amacrine cells, and ganglion cells. Amacrine cells receive excitatory glutamatergic input from bipolar cells and primarily inhibitory input from other amacrine cells (Masland, 2001). The bipolar cells are differentiated at a late of gestational period (Hollenberg & Spira, 1973). Through its developmental stage, the bipolar cells become numerous and occupy the majority of the INL. Two types of bipolar cells are detected: large pale cells and small dark ones. Cohen and Sterling (1990) interpret that the larger cells are cone bipolar cells, while MacNeil et al. (2009) detected that the smaller, sclerally placed cells are rod bipolar cells. The bipolar cells connect the inner and outer

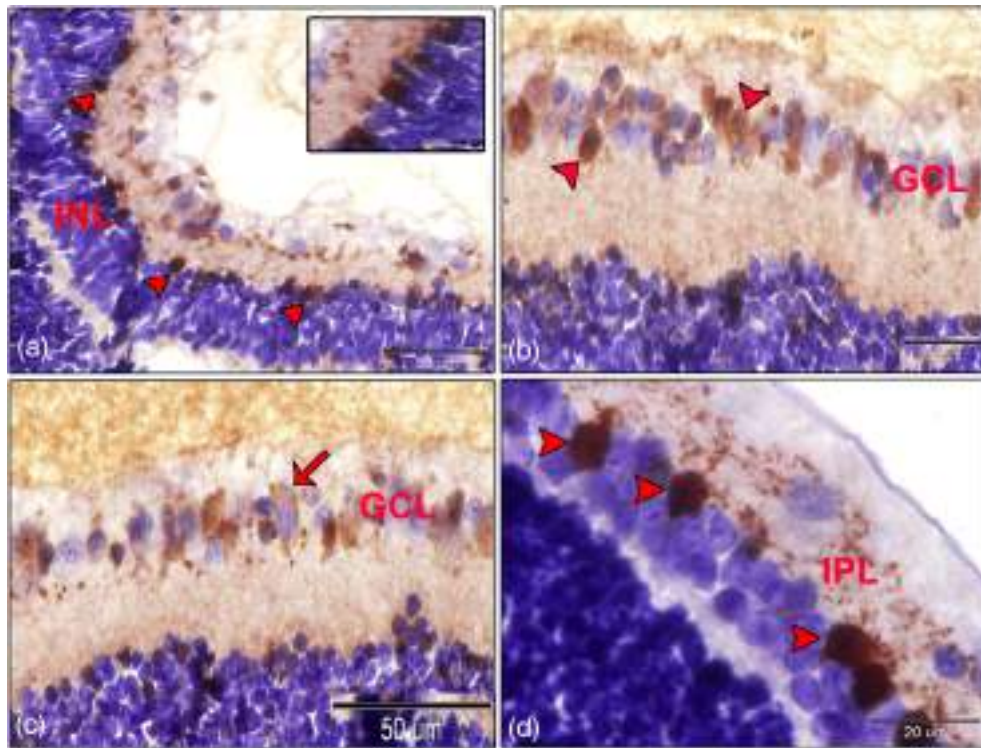


FIGURE 9 S100 immunostained sections of the developing rabbit retina on the second week (a, b) and the first month (c, d) after birth. (a) Showing strong positive reaction for S100 protein in the cell bodies of Muller cells (arrowheads) within the inner nuclear layer (INL). (b) Positively stained satellite glial cells (arrows) surrounding the ganglionic cells (zigzag arrow) which showed negative immunoreactivity. (c) Shows the S100 immunoreactivity expressed in different layers of the retina. Inner limiting membrane (arrowhead), nerve fiber layer (arrow), inner plexiform layer (IPL), inner nuclear layer (INL), outer nuclear layer (ONL), and outer limiting membrane (zigzag arrow). (d) Shows the immunoreactive processes (arrowheads) of Muller cells (arrows) extend between the cells of the outer nuclear layer (ONL) till reach the outer limiting membrane (zigzag arrow) that expressed positive reaction for S100.

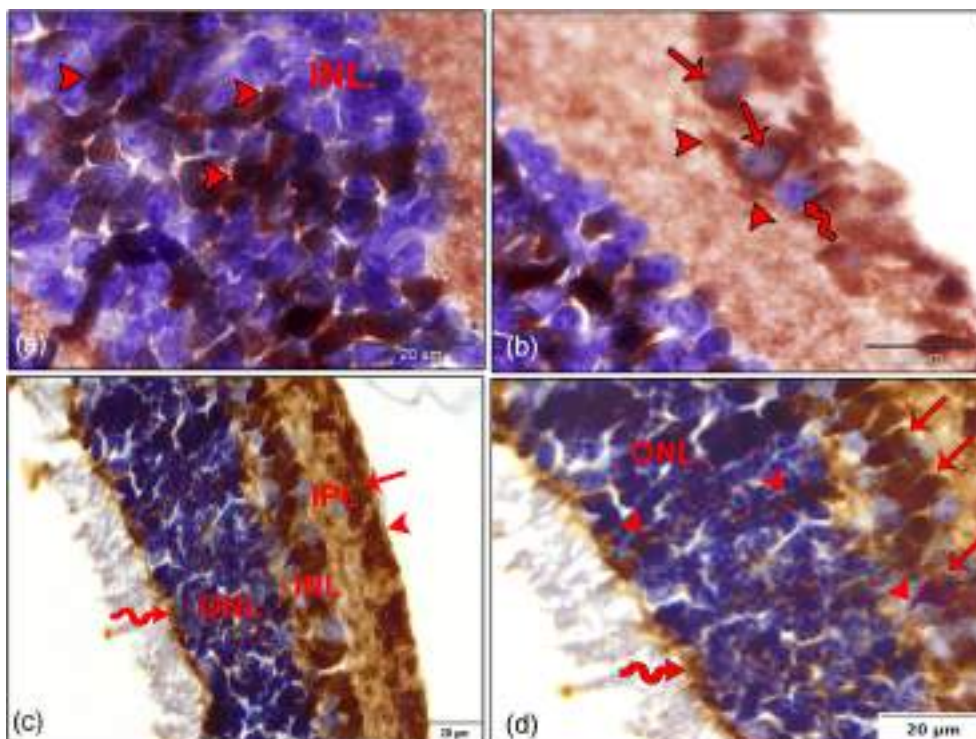


FIGURE 10 Calretinin immunostained sections of the developing rabbit retina on the first week (a–c) and the first month (d) after birth showing strong positive reaction for calretinin in the nucleus and cytoplasm of the amacrine cells (arrowheads) within the inner nuclear layer (INL) and the displaced amacrine cells (zigzag arrows) in the ganglionic cell layer (GCL). Ganglionic cells exhibited moderate immunoreactivity for calretinin confined to their cytoplasm (arrow). Take note of the positively stained meshwork within the inner plexiform layer (IPL).

TABLE 3 Developmental timetable of differentiation of the cellular components and the layers of the rabbit retina.

Age	Developmental events
10th day of gestation	Formation of optic cup.
11th day	Differentiation of pigmented layer of the retina.
13th day	The pars theca and pars optica are distinguished.
15th day	Differentiation of the ganglionic cells.
16th day	Formation of nerve fiber layer.
20th day	Formation of ganglionic cell layer and inner plexiform layer.
23rd day	Appearance of inner limiting membrane, differentiation of Muller, amacrine, and cone cells.
27th day	Differentiation of bipolar cells.
30th day	Formation of inner nuclear layer, outer nuclear layer, outer plexiform layer, and outer limiting membrane. Differentiation of horizontal and rod cells. Differentiation of inner segments of photoreceptors.
One week postnatal	Differentiation of outer segments of photoreceptors. The inner segments are more developed and could be divided two parts: inner myoid and outer ellipsoid.
Two weeks and one month	All layers are established.

retina that act as a relay stations for visual signals (Germain et al., 2010).

The horizontal cells appear at end of gestational period, and its appearance resulting the neuroblastic cell layer is divided into the INL and ONL. In agreement with Soliman et al. (2010) in goat, the processes of the horizontal cells run in parallel to the retinal surface. The horizontal cells are interneurons that involved in enhancing contrast between light and dark regions (Edqvist, 2006). Loss of the horizontal cells in the developing stage causes defects in the retinal layer structure as well as in photoreceptor ribbon synapse formation (Keeley et al., 2013; Wu et al., 2013). The OPL is a faint line and forms by the horizontal cells and their processes that extended in horizontal plane. Then, it becomes a distinct layer where the processes of photoreceptor cells communicate with the processes of the horizontal, amacrine, and bipolar cells (Gupta, Kapoor, et al., 2016).

The ONL contains two types of photoreceptor cell bodies: rod and cone cells. The cone cells are differentiated earlier and more active than the rod cells, and this result is agreed with Nag and Wadhwa (2001) in human, Derbalah (2001) in camel, and Aly (2003) in bovine. The photoreceptors are responsible for converting light into neuronal signals. Rods are mainly involved in vision under dim light conditions, whereas the cones are normally involved in vision during bright light and are also responsible for color vision (Edqvist, 2006). The outer limiting membrane is formed by a series of zonula adherens

between the Muller cell processes and the photoreceptors (Soliman et al., 2010). It is believed that this type of junction binds cells less firmly than do desmosomes or zonula occludens (Lentz & Trinkaus, 1971) and permits the passage of some materials between the cells (Peyman et al., 1971). The inner limiting membrane is formed before the outer limiting membrane. The late in differentiation of the outer processes has been observed previously (Hollenberg & Spira, 1973; Rhodes, 1979).

The inner segments of the photoreceptors divided into inner myoid and outer ellipsoid parts. The abundant of mitochondria in the outer ellipsoid part considers source of energy for the high metabolic activity of the cones (Aly, 2003) and associated with active sodium pump in the rods (Hagins, 1973). Braekevelt (1973) observed the basal bodies of the connecting cilium between the inner and outer segments. It considered a constant feature of all photoreceptors described. In agreement with Greiner and Weidman (1982) in rabbit, the outer segments of the photoreceptors are not seen during prenatal development. The function of the outer segment of the photoreceptors is absorption of the light through the photopigments (transmembrane proteins) and converting it into electrical signals in a process known as phototransduction (Molday & Moritz, 2015). The inner segments are responsible for metabolism and regulation of electrical signals (Baker & Kerov, 2013).

The expression of S100 protein in different layers of the retina was studied, and S100 protein is expressed in the Muller cells. S100 protein is considered an acidic Ca²⁺-binding protein, where it is localized primarily in the nucleus and cytoplasm of Muller cells. The function of the S100 protein is to regulate the cellular processes as differentiation, proliferation, inflammation, apoptosis, migration, and invasion, energy metabolism, and Ca²⁺ homeostasis. So, the S100 protein is a useful tool in studying the cytoarchitecture of the normal retina as well as the pathological conditions (Gonzalez et al., 2020). Although large number of Muller cells expressed S100, some Muller cells had negative immunoreactivity. The lack of S100 immunoreactivity in some Muller cells of the rabbit retina may be due to the amounts of S100 in some Muller cells are too small to be detectable immunohistochemically (Sehntzer, 1987). S100 protein is present in chicken retina as well as in Muller cells and astrocytes of the rabbit retina. It is not found in human retina; therefore, the immunohistochemical staining for S100 protein can be used to study pathologic conditions in the Muller cells of retina in guinea pig, hamster, rat, and rabbit, but it has limited value in investigations of the same conditions in human eye (Molnar et al., 1984).

The immunolocalization of the calretinin in the rabbit retina is studied. Calretinin is one of EF-hand calcium-binding protein family that has been shown to be present in most nerve cells (Baimbridge et al., 1992). We revealed that very intense calretinin immunoreactivity could be observed in the amacrine cells which occupy the most inner row of inner nuclear layer. Similar observation was recorded by Völgyi et al. (1997). In addition to the immunoreactive amacrine cells, the ganglionic cell layer also showed positive immunoreactivity to calretinin. These cells are ganglion cells and displaced amacrine cells. In agreement with Völgyi et al. (1997), the amacrine cells show very

strong immunoreactivity, while the ganglionic cells express less immunoreactivity to calretinin. Calretinin plays an important role in retinal development and the differentiation and maturation of horizontal, amacrine, and ganglion cells (Ellis et al., 1991; Nag & Wadhwa, 1999). It also regulates the ganglion cell axon outgrowth during development and regeneration after injury (García-Crespo & Vecino, 2004).

The different immunohistochemical markers are used for the retinal cell types. The neurofilament 68 is used for detecting the nerve fiber layer. For large ganglion cells, the glucose-regulated protein 78 is applied (Deeg et al., 2006), while the axons of the ganglion cells are positive for neurofilament protein (Yuge et al., 1995). The vimentin, glial fibrillary acidic protein (GFAP), and glutamine synthetase (GS) are the specific antibodies that stain the proteins of Muller glial cells (Deeg et al., 2006). In addition to the S100 protein, GFAP and vimentin are detected in astrocytes and Muller cells (Yuge et al., 1995). The syntaxin expression is specific for amacrine cells in mammalian species (Barnstable et al., 1985). Also, the inner plexiform layer is syntaxin positive. The synaptophysin is seen in both plexiform layers. The neuron-specific enolase (NSE) is expressed in bipolar, ganglion, and photoreceptor cells and in their cell processes (Yuge et al., 1995). The NSE is also used for detection of horizontal cells (Deeg et al., 2006). Parvalbumin immunoreactivity is reacted for subpopulations of bipolar, ganglion, horizontal, and amacrine cells in different species (Sanna et al., 1993). In addition, the bcl-2 oncoprotein is reacted in ganglion and bipolar cells (Yuge et al., 1995). The rod bipolar cells are stained by antibodies against protein kinase C (PKC) in some vertebrates. The outer segments of photoreceptor are reacted with transducin and retinal S-antigen (Deeg et al., 2006).

In conclusion, the process of neuro- and gliogenesis in the rabbit retina occurs in several stages. All these stages take place during the embryonic period, while the outer segments of the photoreceptors are developed on the first week of age postnatally. Interestingly, rabbits are born blind; the eyes open and the retina becomes functional by the second week of life when the last component of the retina, the outer segments of the photoreceptors which are responsible for phototransduction and initiating the process of vision, develops. Taken all together, development of the retina takes place in a precise sequence and any disturbance in this order may cause vision impairment. The significance of the current study was to investigate the timing of differentiation and development of the different cell components of the retina. Therefore, future research should focus on the early detection of the retinal malformations and abnormalities before the end of the gestation period.

AUTHOR CONTRIBUTIONS

Sara El-Desoky: Methodology; writing – review and editing; conceptualization; investigation. **Ruwaida Elhanbaly:** Methodology; conceptualization; investigation. **Abdalla Hifny:** Conceptualization; investigation; writing – review and editing. **Nagwa Ibrahim:** Writing – original draft; methodology; writing – review and editing; investigation. **Wafaa Gaber:** Writing – review and editing; methodology; investigation; conceptualization.

ACKNOWLEDGMENTS

The authors thank the Electron Microscopy Unit technicians at Assiut University for their help in processing the imaging of the electron microscopy samples.

FUNDING INFORMATION

This research did not receive any specific grant from any funding agency in the public, commercial, or not-for-profit sector.

CONFLICT OF INTEREST STATEMENT

The authors declare no conflict of interest.

DATA AVAILABILITY STATEMENT

The data that support the findings of this study are available from the corresponding author upon reasonable request.

ORCID

Wafaa Gaber  <https://orcid.org/0000-0003-1754-8489>

REFERENCES

- Abd-Elhafeez, H. H., & Soliman, S. A. (2017). New description of telocyte sheaths in the bovine uterine tube: An immunohistochemical and scanning microscopic study. *Cells Tissue Organs*, 203, 295–315.
- Abd-Elkareem, M. (2017). Cell-specific immuno-localization of progesterone receptor alpha in the rabbit ovary during pregnancy and after parturition. *Animal Reproduction Science*, 180, 100–120.
- Abdel-Maksoud, F. M., Abd-Elhafeez, H. H., & Soliman, S. A. (2019). Morphological changes of telocytes in camel efferent ductules in response to seasonal variations during the reproductive cycle. *Scientific Reports*, 9, 1–17.
- Aly, K. (2003). *Glycohistochemical, immunohistochemical and electron microscopic examination of the bovine eyeball*. PhD thesis, Faculty of Veterinary Medicine, Ludwig-Maximilians-Munich University.
- Baimbridge, K. G., Celio, M. R., & Rogers, J. H. (1992). Calcium-binding proteins in the nervous system. *Trends in Neurosciences*, 15, 303–308.
- Baker, S. A., & Kerov, V. (2013). Photoreceptor inner and outer segments. *Current Topics in Membranes*, 72, 231–265.
- Bancroft, J. D., Layton, C., & Suvarna, S. K. (2013). *Bancroft's theory and practice of histological techniques* (7th ed.). Elsevier/Churchill Livingstone.
- Barnstable, C. J., Hofstein, R., & Akagawa, K. (1985). A marker of early amacrine cell development in rat retina. *Brain Research*, 352, 286–290.
- Bhattacharjee, J., & Sanyal, S. (1975). Developmental origin and early differentiation of retinal Müller cells in mice. *Journal of Anatomy*, 120, 367.
- Boycott, B. B., & Wassle, H. (1974). The morphological types of ganglionic cells in the domestic cat's retina. *The American Journal of Physiology*, 226, 397–400.
- Braekevelt, C. R. (1973). Fine structure of the retinal pigment epithelium and photoreceptor cells on an Australian marsupial Setonix brachyurus. *Canadian Journal of Zoology*, 51, 1093–1100.
- Carlson, B. M. (1985). *Patten's foundations of embryology* (4th ed.). Tata McGraw-Hill Publishing Company Ltd.
- Cohen, E., & Sterling, P. (1990). Demonstration of cell types among cone bipolar neurons of cat retina. *Philosophical Transactions of the Royal Society of London. Series B: Biological Sciences*, 330, 305–321.
- Deeg, C. A., Amann, B., Hauck, S. M., & Kaspers, B. (2006). Defining cytochemical markers for different cell types in the equine retina. *Anatomia, Histologia, Embryologia*, 35, 412–415.

- Derbalah, A. E. M. (2001). Light and electron microscopical studies on the eye of one-humped camel (*Camelus dromedaries*). MVSc. Thesis. Alex. Univ., Fac. Vet. Med. Cytol. Histol. Dept. Acta Soc. Ophthalmol., 84, 1376–1384.
- Edqvist, P. H. (2006). Neuronal development in the embryonic retina: Focus on the characterization, generation and development of horizontal cell subtypes. *Acta Universitatis Upsaliensis*, 170, 1–83.
- Ehrenhofer, M. C., Deeg, C. A., Reese, S., Liebich, H. G., Stangassinger, M., & Kaspers, B. (2002). Normal structure and age-related changes of the equine retina. *Veterinary Ophthalmology*, 5, 39–47.
- Ellis, J., Richards, D., & Rogers, J. (1991). Calretinin and calbindin in the retina of the developing chick. *Cell and Tissue Research*, 264, 197–208.
- Fischer, A. J., & Bongini, R. (2010). Turning Müller glia into neural progenitors in the retina. *Molecular Neurobiology*, 42, 199–209.
- García-Crespo, D., & Vecino, E. (2004). Differential expression of calretinin in the developing and regenerating zebrafish visual system. *Histology and Histopathology*, 19, 1193–1199.
- Germain, F., Perez-Rico, C., Vicente, J., & de la Villa, P. (2010). Functional histology of the retina. *Microscopy: Science, Technology, Applications and Education*, 914–925.
- Gonzalez, L. L., Garrie, K., & Turner, M. D. (2020). Role of S100 proteins in health and disease. *Biochimica et Biophysica Acta (BBA)-Molecular Cell Research*, 1867, 1–16.
- Greiner, J. V., & Weidman, T. A. (1981). Histogenesis of the ferret retina. *Experimental Eye Research*, 33, 315–332.
- Greiner, J. V., & Weidman, T. A. (1982). Embryogenesis of the rabbit retina. *Experimental Eye Research*, 34, 749–765.
- Gupta, M. P., Herzlich, A. A., Sauer, T., & Chan, C. C. (2016). Retinal anatomy and pathology. *Retinal. Pharmacotherapy*, 55, 7–17.
- Gupta, T., Kapoor, K., Sahni, D., & Singh, B. (2016b). Mapping the time line of development in each layer of human foetal retina. *Journal of Clinical and Diagnostic Research*, 10, AC04–AC07.
- Gwon, A. (2008). The rabbit in cataract/IOL surgery models in eye. In P. Tsonis (Ed.), *Animal Research* (pp. 184–204). Academic Press.
- Hagins, W. A. (1973). The visual process. *Annual Review of Biophysics and Bioengineering*, 1, 131–158.
- Harman, A., Dann, J., Ahmat, A., Macuda, T., Johnston, K., & Timneyb, B. (2001). The retinal ganglion cell layer and visual acuity of the camel. *Brain, Behavior and Evolution*, 58, 15–27.
- Haruta, M., Sasai, Y., Kawasaki, H., Amemiya, K., Ooto, S., Kitada, M., Suemori, H., Nakatsuji, N., Ide, C., & Honda, Y. (2004). In vitro and in vivo characterization of pigment epithelial cells differentiated from primate embryonic stem cells. *Investigative Ophthalmology and Visual Science*, 45, 1020–1025.
- Hitchcock, P. F., & Raymond, P. A. (2004). The teleost retina as a model for developmental and regeneration biology. *Zebrafish*, 1, 257–271.
- Hollenberg, M. J., & Spira, A. W. (1973). Human retinal development: Ultrastructure of the outer retina. *The American Journal of Anatomy*, 137, 357–385.
- Karnovsky, M. J. (1965). A formaldehyde glutaraldehyde fixative of high osmolality for use in electron microscopy. *The Journal of Cell Biology*, 27, 137.
- Keeley, P. W., Luna, G., Fariss, R. N., Skyles, K. A., Madsen, N. R., Raven, M. A., Poché, R. A., Swindell, E. C., Jamrich, M., & Oh, E. C. (2013). Development and plasticity of outer retinal circuitry following genetic removal of horizontal cells. *The Journal of Neuroscience*, 33, 17847–17862.
- Komáromy, A. M. (2010). Day blind sheep and the importance of large animal disease models. *Veterinary Journal*, 185, 241–242.
- Kurata, M., Yamagiwa, Y., Haranosono, Y., & Sakaki, H. (2017). Repeated-dose ocular instillation toxicity study: A survey of its study design on the basis of common technical documents in Japan. *Fundamental Toxicological Sciences*, 4, 95–99.
- Kuwabara, T., & Weidman, T. (1974). Development of the prenatal rat retina. *Investigative Ophthalmology and Visual Science*, 13, 725–739.
- Lentz, T. L., & Trinkaus, J. (1971). Differentiation of the junctional complex of surface cells in the developing Fundulus blastoderm. *The Journal of Cell Biology*, 48, 455–472.
- MacNeil, M. A., Purrier, S., & Rushmore, R. (2009). The composition of the inner nuclear layer of the cat retina. *Visual Neuroscience*, 26, 365–374.
- Masland, R. H. (2001). The fundamental plan of the retina. *Nature Neuroscience*, 4, 877–886.
- McGeady, T., Quinn, P., Fitzpatrick, E. S., & Ryan, M. (2006). *Veterinary embryology* (1st ed.). Blackwell Publishing.
- Miyata, T. (2008). Development of three-dimensional architecture of the neuroepithelium: Role of pseudostratification and cellular community. *Development, Growth & Differentiation*, 50, 105–112.
- Molday, R. S., & Moritz, O. L. (2015). Photoreceptors at a glance. *Journal of Cell Science*, 128, 4039–4045.
- Molnar, M., Stefansson, K., Marton, L. S., Tripathi, R. C., & Molnar, G. K. (1984). Distribution of S100 protein and glial fibrillary protein in normal and gliotic human retina. *Experimental Eye Research*, 38, 27–34.
- Moshiri, A., Close, J., & Reh, T. A. (2004). Retinal stem cells and regeneration. *The International Journal of Developmental Biology*, 48, 1003–1014.
- Nag, T., & Wadhwa, S. (1999). Developmental expression of calretinin immunoreactivity in the human retina and a comparison with two other EF-hand calcium-binding proteins. *Neuroscience*, 91, 41–50.
- Nag, T., & Wadhwa, S. (2001). Differential expression of syntaxin-1 and synaptophysin in the developing and adult human retina. *Journal of Biosciences*, 26, 179–191.
- Peyman, G. A., Spitznas, M., & Straatsma, B. R. (1971). Peroxidase diffusion in the normal and photocoagulated retina. *Investigative Ophthalmology and Visual Science*, 10, 181–189.
- Rapaport, D. H., Wong, L. L., Wood, E. D., Yasumura, D., & LaVail, M. M. (2004). Timing and topography of cell genesis in the rat retina. *The Journal of Comparative Neurology*, 474, 304–324.
- Reynolds, E. S. (1963). The use of lead citrate at high pH as an electron-opaque stain in electron microscopy. *The Journal of Cell Biology*, 17, 208–212.
- Rhodes, R. H. (1979). A light microscopic study of the developing human neural retina. *The American Journal of Anatomy*, 154, 195–209.
- Sanna, P. P., Keyser, K. T., Celio, M. R., Karten, H. J., & Bloom, F. E. (1993). Distribution of parvalbumin immunoreactivity in the vertebrate retina. *Brain Research*, 600, 141–150.
- Sehnitzer, J. (1987). Immunocytochemical localization of S-100 protein in astrocytes and muller cells in the rabbit retina. *Cell and Tissue Research*, 248, 55–61.
- Sernagor, E., Eglén, S., Harris, B., & Wong, R. (2006). *Retinal neurogenesis*. Cambridge University Press.
- Shara, B., Adhami, M., & Amr, M. (2013). A comparison of routine fixation and microwave fixation of the retina in *Garrarufa*. *International Journal of Current Science*, 5, 101–108.
- Soliman, S., Adam, Z., & Abd Allah, U. (2010). Light and electron microscopic structure of goat's retina. *Journal of Veterinary Medical Research*, 20, 52–62.
- Toft-Kehler, A. K., Skytt, D. M., Svare, A., Lefever, E., Van Hove, I., Moons, L., Waagepetersen, H. S., & Kolko, M. (2017). Mitochondrial function in Müller cells—does it matter? *Mitochondrion*, 36, 43–51.
- Tomar, M. P. S., & Bansal, N. (2019). Prenatal development of retina in buffalo (*Bubalus bubalis*). *Anatomia, Histologia, Embryologia*, 48, 125–132.
- Tworig, J. M., & Feller, M. B. (2021). Müller glia in retinal development: From specification to circuit integration. *Frontiers in Neural Circuits*, 15, 815–923.
- Völgyi, B., Pollák, E., Buzás, P., & Gábel, R. (1997). Calretinin in neurochemically well-defined cell populations of rabbit retina. *Brain Research*, 763, 79–86.
- Walling, B. E., & Marit, G. B. (2016). The eye and harderian gland. In *Atlas of histology of the juvenile rat* (pp. 373–394). Elsevier.
- Walsh, C., & Polley, E. (1985). The topography of ganglion cell production in the cat's retina. *The Journal of Neuroscience*, 5, 741–750.

- Wassle, H., & Boycott, B. B. (1991). Functional architecture of the mammalian retina. *Physiological Reviews*, *71*, 447–480.
- Wu, F., Li, R., Umino, Y., Kaczynski, T. J., Sapkota, D., Li, S., Xiang, M., Fliesler, S. J., Sherry, D. M., & Gannon, M. (2013). Onecut1 is essential for horizontal cell genesis and retinal integrity. *The Journal of Neuroscience*, *33*, 13053–13065.
- Yuge, K., Nakajima, M., Uemura, Y., Miki, H., Uyama, M., & Tsubura, A. (1995). Immunohistochemical features of the human retina and retinoblastoma. *Virchows Archiv*, *426*(6), 571–575. <https://doi.org/10.1007/BF00192111>

How to cite this article: El-Desoky, S. M. M., Elhanbaly, R., Hifny, A., Ibrahim, N., & Gaber, W. (2023). Temporospatial dynamics of the morphogenesis of the rabbit retina from prenatal to postnatal life: Light and electron microscopic study. *Microscopy Research and Technique*, 1–16. <https://doi.org/10.1002/jemt.24466>